RSC Advances


This is an *Accepted Manuscript*, which has been through the Royal Society of Chemistry peer review process and has been accepted for publication.

*Accepted Manuscripts* are published online shortly after acceptance, before technical editing, formatting and proof reading. Using this free service, authors can make their results available to the community, in citable form, before we publish the edited article. This *Accepted Manuscript* will be replaced by the edited, formatted and paginated article as soon as this is available.

You can find more information about *Accepted Manuscripts* in the Information for Authors.

Please note that technical editing may introduce minor changes to the text and/or graphics, which may alter content. The journal's standard Terms & Conditions and the Ethical guidelines still apply. In no event shall the Royal Society of Chemistry be held responsible for any errors or omissions in this *Accepted Manuscript* or any consequences arising from the use of any information it contains.

ROYAL SOCIETY OF CHEMISTRY

www.rsc.org/advances

Please do not adjust margins

RSC Advances

COMMUNICATION

# Single Particle Electrochemistry of *p*-Hydroxythiophenol-labeled Gold Nanoparticles

Received 00th January 20xx,
Accepted 00th January 20xx

DOI: 10.1039/x0xx00000x

www.rsc.org/

Jing Zhang, Yongfeng Wei,* Lei Tian and Xiaofeng Kang*

**In the communication, we assembled an electroactive *p*-hydroxythiophenol (*p*-HTP) monolayer on a gold nanoparticle surface and produced an amplified single particle-collision electrochemical signal, thus allowing us to sensitively detect the size and functions of inert gold particles in aqueous solution.**

Gold nanoparticle (AuNP) has drawn great attention in its applications including optics,[1] medicine,[2,3] catalysts[4] and sensors[5,6] due to its extraordinary physical and chemical properties. However, these properties are strongly dependent on their size and aggregation state in addition to structure and composition. The properties of single metal NPs are distinct from that of a large number of NPs or the NPs ensemble. For example, different catalytic activity was observed between individual electrocatalyst particles and its aggregates.[7] In many cases, we need to monitor and evaluate the behaviors of single NP, or even functionalized single NP, such as those used as single NP probes[8,9] and single NP sensors.[10-12] However, it remains a challenge to develop a technique that can directly, rapidly and simply measure the electrochemical activity of single particles.

Some methods have been reported for this purpose including scanning electrochemical microscopy (SECM),[13] plasmonic-based electrochemical current imaging (P-ECI),[14] high-resolution fluorescence microscopy[15] and particle collision electrochemistry.[16-25] The last one is the simplest, yet most effective method for characterizing single particles. The principle is based on the detection of tiny current spike produced by individual NP's collision with ultramicroelectrode. The transient current event in collision is associated with either the redox of NP itself[16-20] or a NP-catalyzed reaction[21-25]. This technique has been successfully employed to detect different types of NPs including metal (silver,[16] nickel,[17] and copper[18]), metal oxide ($Fe_3O_4$)[19] and organic NPs (indigo)[20]. However, its availability is restricted to NPs that possess electrochemical activity, for which the oxidation or reduction is able to take place at the electrode surface. On the other hand, the collision current is often very small, thus limiting its detection sensitivity. One of the strategies to improve detection is to amplify the current signal through particle-catalyzed reaction, in which a higher sensitivity can be achieved by measuring the transient electrocatalytic current of single NPs colliding on an electrode surface.[21-25] For example, the platinum NP-electrocatalyzed reaction can amplify about 10 orders of magnitude in the current.[21]

In general, it is difficult to directly characterize and detect AuNPs in aqueous solution at single particle level using simple methods.[26] Due to non-electrochemical activity, particle collision electrochemistry also can't be used to analyze AuNPs under mild condition.[27] In the communication, a single layer of *p*-hydroxythiophenol (*p*-HTP) was self-assembled on AuNPs surface to form electroactive *p*-HTP-AuNPs. As illustrated in scheme 1, the functionalized AuNPs not only can generate single particle collision signal through the oxidation of *p*-HTP, but also induce an amplified transient current due to a large number of conjugated HTP molecules modified on AuNPs. During the collision of *p*-HTP-AuNPs with ultramicroelectrode,the electrons can be effectively transferred to produce characteristic current-time signal, which allows us to identify and detect AuNPs, and even their functions.

The citrate-capped AuNPs and *p*-HTP-functionalized AuNPs were prepared by a revising previous protocol (for details see SI).[28,29] Briefly, 1.7 mL of 1.0 % trisodium citrate solution was quickly added to 31.7 mL of boiled 0.01 % $HAuCl_4$ solution under vigorous stirring. The color change from pale yellow to deep red indicated the

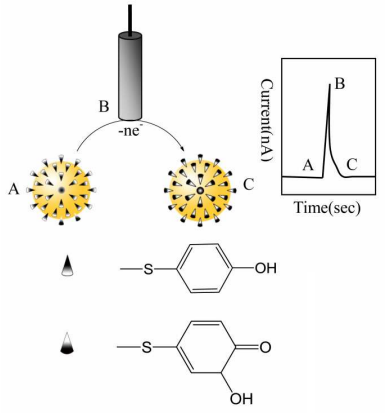


**Scheme 1** The collision process and the signal response of *p*-HTP-AuNPs on CFMDE

*Key Laboratory of Synthetic and Natural Functional Molecular Chemistry, College of Chemistry & Materials Science, Northwest University, Xi'an 710069, P. R. China. E-mail: kangxf@nwu.edu.cn, Fax: +86-029-88302604.

† Electronic Supplementary Information (ESI) available: Experimental procedure, nanoparticle preparation and characterization. See DOI: 10.1039/b000000x

RSC Advances Accepted Manuscript

formation of AuNPs. Followed by continuous stirring and cooling down, the excess trisodium citrate was removed by centrifugation and wash three times with ultrapure water. The resulting citrate-capped AuNPs (denoted as C-AuNPs) solution was stored at 4 °C in the dark. *p*-HTP-functionalized AuNPs (denoted as *p*-HTP-AuNPs) were obtained by ligand exchanging between citrate and *p*-HTP. In the process, 2.0 mL of 5 mM *p*-HTP was added drop-by-drop into2.0 mL of 3.2 x $10^{-9}$ mol/L C-AuNPs, and stirred for 24 h at room temperature. By centrifugation at 8000 rpm, excessive free ligands were removed until no *p*-HTP was detected in the leacheate. The purified product was redispersed in ultrapure water and stored at 4 °C.

Transmission electron microscope (TEM), Fourier transform infrared spectra (FT-IR) and UV-Vis spectroscopy were used to characterize these NPs. Fig. S1 is two representative TEM micrographs of C-AuNPs and *p*-HTP-AuNPs. The average diameter of AuNPs was between 14 nm and 18 nm with a narrow size distribution (see the insets of Fig. S1). As reported previously,[30,31] these NPs showed the geometric shape of truncated decahedron or truncated octahedron. Both C-AuNPs and *p*-HTP-AuNPs were quite uniform, and the size and morphology remained unchanged after the ligand exchange. FT-IR analysis (Fig. S2 and SI) demonstrated the presence of *p*-HTP on *p*-HTP-AuNP. UV-Vis spectroscopic studies were performed at room temperature from 300 to 800 nm. The typical common absorption feature was observed for C-AuNPs and *p*-HTP-AuNPs, such as an exponential decay with increasing wavelength (Mie scattering) onto which a surface plasmon band at 520 nm (due to the inter-band transition of the gold core 5d electrons) was superimposed (Fig. S3), and one can easily see that the surface plasma resonance band doesn't shift after the exchange of the surface passivation ligand. This indicates that the size of the AuNPs before and after the surface ligands exchange remained unchanged. To explore the working conditions of single particle-collision electrochemistry, the electrochemical behavior of the modified electrodes with C-AuNPs and *p*-HTP-AuNPs were studied. The experiments were performed in a Faraday cage with an electrolyte containing 50 mM sodium dihydrogen citrate and 90 mM potassium chloride. Cyclic voltammograms (CV) and differential pulse voltammograms (DPV) were recorded using a three-electrode system: a glassy carbon electrode (GCE, the working electrode) loaded with C-AuNPs or *p*-HTP-AuNPs, a Pt counter electrode and an Ag/AgCl reference electrode. To prepare the NPs-modified GCEs, a 5 µL of suspension of C-AuNPs or *p*-HTP-AuNPs (ca. $10^{14}$ particles $dm^{-3}$) was drop-cast on GCE and left to dry under $N_2$ atmosphere. From the CV curves (Fig. S4), no featured electrochemical response was observed on both the naked GCE (black curve) and the C-AuNPs modified GCE (red curve). However, in the case of GCE modified with *p*-HTP-AuNPs, there was a pair of distinct redox peaks (magenta curve) at 0.4 V and 0.95 V. Similar results were obtained from DPV (no shown).

Particle-collision electrochemical experiments were conducted on a prepared carbon fiber microdisk electrode (CFMDE) with a radius of 3.5 µm. C-AuNPs or *p*-HTP-AuNPs were pre-dispersed in 50 mM of citrate solution. The potential was held at 1.4 V (vs. Ag/AgCl electrode) and the oxidative transient current was recorded using a Picoammeter with a Faraday cage system (Keithley, Keithley Instruments Inc.). We observed that larger current spikes from the current-time trace for *p*-HTP-AuNPs (curve d in Fig. 1), and no spike signals for the blank controlling solution (curve a in Fig. 1) and C-AuNPs (curve b in Fig. 1). The results demonstrated that *p*-HTP-functionalized AuNPs are electrochemically active, which can be used to study the electrochemical process of NPs at single particle level.

A spike signal in a characteristic current-time curve corresponds to a single particle-collision event. The area of a sharp spike can be integrated to calculate charge exchanged on the electrode surface in each particle collision. Interestingly, based on the analysis of 300 events, the charge transferred between the electrode and *p*-HTP-AuNP in a single particle-collision event is the range of (1.1 ± 0.2) x $10^{-11}$ C to (5.2 ± 0.4) x $10^{-11}$ C for 14 nm ~ 18 nm of particles, which is far higher than other NPs systems, for example, 13 nm of AgNPs in the citrate solution (6.9 x $10^{-13}$ C) and 15 nm of AuNPs in 0.1 M HCl (4.0 x $10^{-13}$ C).[16,27] A possible explanation is that strong S-Au covalent bond and aromatic ring facilitate the electron exchange between NPs and electrode.

To explore the origination, a control experiment of 1-pentanethiol-AuNPs (AuNPs labeled with 1-pentanethiol) was conducted under the same conditions. The current-time trace (Fig. 1, curve c) is a featureless exponential decay. Similar result was obtained in another control experiment of thiophenol-AuNPs (no shown). These experiments demonstrated that the oxidation current spike of *p*-HTP-AuNP stems from the hydroxyl oxidation in *p*-hydroxythiophenol, rather than S-Au bond, gold core and aromatic ring. Nevertheless, the S-Au bond, gold core and aromatic ring play very important roles for larger transient current as discussed in the following context.

For free *p*-HTP in the solution, no oxidation peak yieldED on the GCE (the blue curve in Fig. S4). But *p*-HTP could be oxidized either on *p*-HTP-AuNPs modified on GCE or when *p*-HTP-AuNPs in the solution occurred in the collision with CFMDE. The AuNPs core with high conductivity is helpful for electrons transfer. The S-Au bond is frequently used in the junctions of molecular wire to link gold electrode to various organic molecules, especially π-conjugated aromatic thiolates that have intrinsic conductivities (in general, they differ by several orders of magnitude compared with non-aromatic

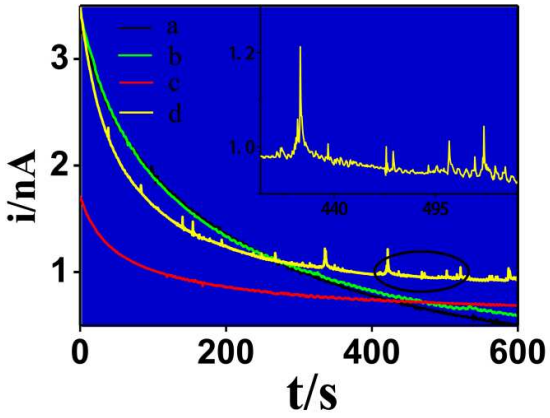


**Fig. 1** Chronoamperometric curves in 50 mM citrate solution. (a) blank solution, (b) C-AuNPs, (c) 1-pentanethiol-AuNPs and (d) p-HTP-AuNPs. Carbon fiber microdisk electrode (3.5 µm in radius) was used as working electrode. The applied potential was 1.4 V (vs. Ag/AgCl). The inset shows the detail in d. All NPs' concentration is 7.95 pM.

RSC Advances Accepted Manuscript


This journal is © The Royal Society of Chemistry 20xx

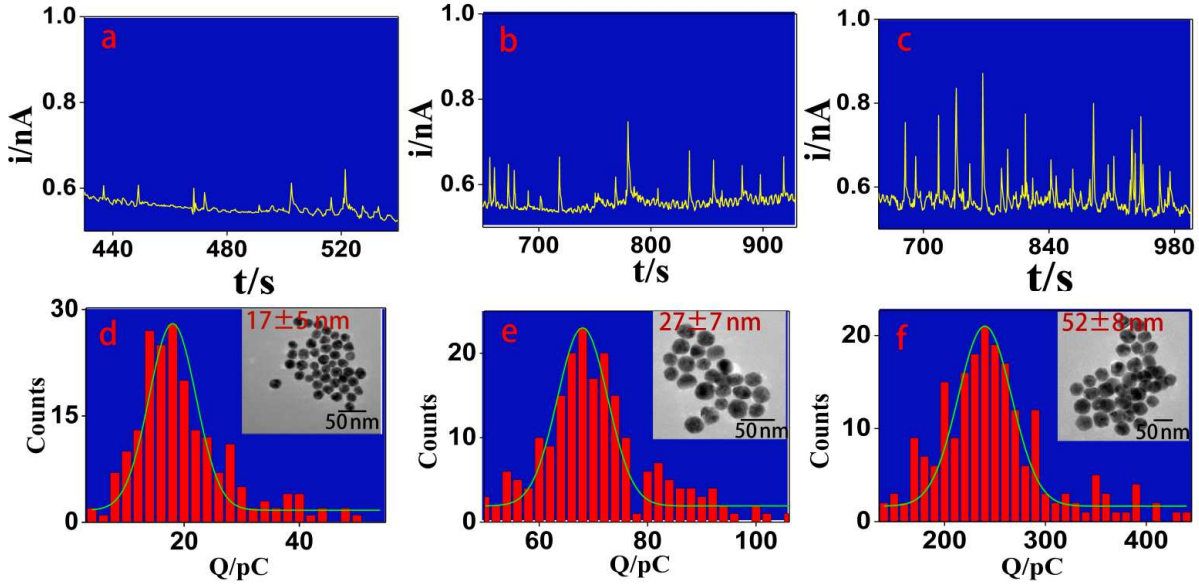


**Fig. 2** Current-time traces recorded for various *p*-HTP-AuNPs (a-c) and corresponding histograms (d-f): (a) and (d) for 17±5 nm in diameter, (b) and (e) for 27±7 nm in diameter, (c) and (f) for 52±8 nm in diameter. The histograms showed the charge distributions. The insets in d-f are TEM images of various *p*-HTP-AuNPs. Other experimental conditions are the same as that in Fig. 1.

compounds).[32] A 16 nm of AuNP can assemble about 8.8x $10^3$ *p*-HTP molecules through the S-Au bond (see SI). All *p*-HTP- molecules on *p*-HTP-AuNP form a unit with the AuNP core. In the unit, electrons can be shared and effectively transferred.

The conclusion is further supported by electrochemical impedance measurement in 0.1 mM KCl containing 5 mM $Fe(CN)_6^{3-/4-}$ (Fig. S5). The double-layer capacitance ($C_{dl}$) of *p*-HTP-AuNPs modified GCE (2.2 μF) is greater than that of C-AuNPs ( 0.95 μF) and 1-pentanethiol-AuNPs (0.85 μF). By $C_{dl} = Q/V$ (Q and V are charge and voltage, respectively), larger capacitance can result in higher electronic charge. The ability of NPs to store electronic charge, namely the capacitance of AuNPs,[33,34] is still highly desirable for the development of particle-based electronic devices.[35, 36]

The electrochemical mechanism of self-assembled layer of *p*-HTP on a gold electrode surface has been studied,[34] which deals with the following two steps (Scheme 2):

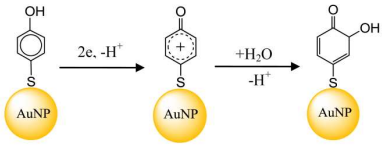


**Scheme 2** The two-electron, two-proton oxidation of *p*-HTP on *p*-HTP-AuNPs.

We therefore proposed a similar pathway for *p*-HTP-AuNPs collision electrochemistry in which 4-Hydroxythiophenol was electrochemically oxidized to quinone with a two electron, two proton reaction mechanism, and involving the formation of carbonium intermediate.

We have demonstrated that *p*-HTP molecules modified on AuNPs have quite significant effects on the properties of AuNPs. The thin singe-layer surrounding the gold core could influence the electron exchange between electrode and AuNPs, out of which an amplified current signal was observed. The larger current will heighten the sensitivity of the detection. Each current spike is associated with individual collision event between the electrode and NPs suspended in an electrolyte. The short-duration transient currents can be further analyzed for determining and sizing the NPs.

According to the relationship between the charge ($Q_t$) and the radius ($R$) of NPs (equation 1),[16] the size distribution of NPs can be obtained.

$$Q_t = \frac{4\pi \cdot f \cdot n_t \cdot e}{S_t} R^2 \qquad (1)$$

Where $f$ is the fractional filling efficiency assuming optimal close-packing of tag moleculars ( 0.91 for spheres on a plane ), $S_t$ is the two-dimensional area occupied by a tag molecular, which can be estimated by the atomic size and the bond length in the *p*-HTP molecular. The parameter $n_t$ is the number of electrons transferred during the oxidation of *p*-HTP-AuNP. $Q_t$ is the charge transferred of every *p*-HTP-AuNPs collide with the microelectrode, $R$ is the radius of NPs. Fig. 2a, 2b and 2c show the current-time trace recordings for various sizes of *p*-HTP-AuNPs. The TEM images were used to confirm the size of *p*-HTP-AuNPs (The insets in Fig. 2d, 2e and 2f). The charge was obtained from the integration of each peak area. We observed that the charge distributions reflected the size distribution of the NPs (Fig. 2d, 2e and 2f). The charge was scaled up linearly with the increased size of the NPs (Fig. S6).

By the slope of $Q_t \sim R^2$ curve (Fig. S6), the number of electrons ($n_t$) transferred in the collision of individual *p*-HTP-AuNP was calculated to be 1.7 x $10^4$. Because the oxidation of individual *p*-HTP needs two electrons, 8.4 x $10^3$ *p*-HTP molecules on a *p*-HTP-AuNPs were oxidized in each collision which is approximately close to the *p*-HTP

RSC Advances Accepted Manuscript

molecular number modified on a AuNP surface ($N_t$ = 8.8 x $10^3$, see SI), supporting the amplified single particle-collision electrochemical signal. In the particle-collision event, individual *p*-HTP-AuNP contacted with ultramicroelectrode, forming single particle nanoelectrode on the ultramicroelectrode, these electrons were thus effectively transferred between the nanoelectrode and the ultramicroelectrode.

Every collision produces a unique current-time event. Event number (collision frequency) is highly correlated with the concentration of *p*-HTP-AuNPs. As presented in Fig. 3 and Fig. 4, the frequency of current spikes increased linearly with the NPs concentration, which can be used to determine the concentration of NPs in the solution.

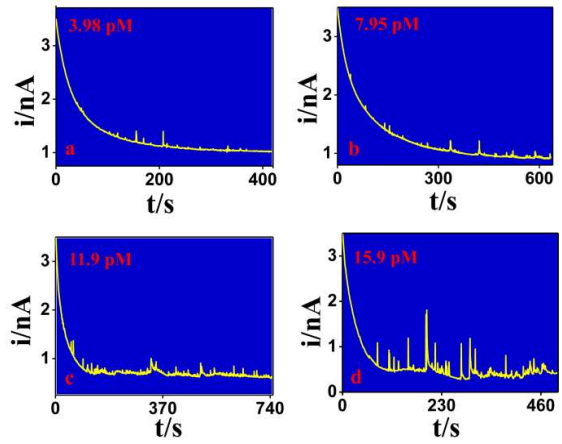


**Fig. 3** Chronoamperometric curves of different concentration of *p*-HTP-AuNPs: (a) 3.98 pM, (b) 7.95 pM, (c) 11.9 pM and (d) 15.9 pM. The potential was held at 1.4 V (vs. Ag/AgCl). A CFMDE working electrode and Ag/AgCl reference electrode were used.

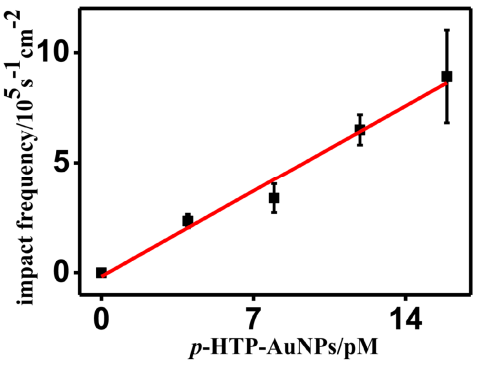


**Fig. 4** Relationship between the impact frequency and the concentration of *p*-HTP-AuNPs.

Here, electroactive *p*-HTP was modified on AuNPs surface through the ligand exchange. The functionalized AuNPs can produce an amplified current spike that allows single particle-collision electrochemistry to readily and sensitively characterize inactivite AuNPs. The strategy of functionalized particles provides a novel route for single particle electrochemical analysis and can extend its application in NPs with non-electrochemical activity.

## Acknowledgements

This work was financially supported by the National ScienceFoundation of China (21175105, 21375104 and 21327806), andthe Specialized Research Fund for the Doctoral Program ofHigher Education of China (20126101110015).

## Notes and references

1 N. Chander, A. F. Khan, E. Thouti, S. K. Sardana, P. S. Chandrasekhar, V. Dutta and V. K. Komarala, *Sol. Energy*, 2014, **109**, 11-23.
2 J. Lee, D. K. Chatterjee, M. H. Lee and S. Krishnan, *Cancer Lett.*, 2014, **347**, 46-53.
3 A. Kumar, H. Ma, X. Zhang, K. Huang, S. Jin, J. Liu, T. Wei, W. Cao, G. Zou and X. -J. Liang, *Biomaterials*, 2012, **33**, 1180-1189.
4 C. Oumahi, J. Lombard, S. Casale, C. Calers, L. Delannoy, C. Louis and X. Carrier, *Catal. Today*, 2014, **235**, 58-71.
5 N. German, A. Ramanavicius and A. Ramanaviciene, *Sens. Actuators B*, 2014, **203**, 25-34.
6 M. Ateeq, M. R. Shah, N. u. Ain, S. Bano, I. Anis, Lubna, S. Faizi, M. F. Bertino and S. S. Naz, *Biosens. Bioelectron.*, 2015, **63**, 499-505.
7 X. Shan, I. Díez-Pérez, L. Wang, P. Wiktor, Y. Gu, L. Zhang, W. Wang, J. Lu, S. Wang, Q. Gong, J. Li and N. Tao, *Nature Nanotech.*, 2012, **7**, 668-672.
8 L. Li, U. Steiner and S. Mahajan, *Nano Lett*., 2014, **14**, 495–498.
9 T. A. Taton, C. A. Mirkin and R. L. Letsinger, *Science*, 2000, **289**, 1757-1760.
10 A. D. McFarland and R. P. V. Duyne, *Nano Lett.*, 2003, **3**, 1057-1062.
11 K. Aslan, M. Wu, J. R. Lakowicz and C. D. Geddes, *J. Am. Chem. Soc.*, 2007, **129**, 1524-1525.
12 C. Wu, B. Bull, K. Christensen and J. McNeill, *Angew. Chem. Int. Ed.*, 2009, **48**, 2741–2745.
13 A. J. Bard, F. -R. F. Fan, D. T. Pierce, P. R. Unwin, D. O. Wipf and F. Zhou, *Science*, 1991, **254**, 68–74.
14 X. Shan, U. Patel, S. Wang, R. Iglesias, and N. Tao, *Science*, 2010, **327**, 1363–1366.
15 X. Zhou, N. M. Andoy, G. Liu, E. Choudhary, K. -S. Han, H. Shen and P. Chen, *Nature Nanotech.*, 2012, **7**, 237–241.
16 N. V. Rees, Y. -G. Zhou and R. G. Compton, Chem. *Phys. Lett.*, 2012, **525-526**, 69-71.
17 E. J. Stuart, Y. -G. Zhou, N. V. Rees and R. G. Compton, *RSC Adv.*, 2012, **2**, 6879-6884.
18 B. Haddou, N. V. Rees and R. G. Compton, *Phys. Chem. Chem. Phys.*, 2012, **14**, 13612-13617.
19 K. Tschulik, B. Haddou, D. Omanović, N. V. Rees and R. G. Compton, *Nano Res.*, 2013, **6**, 836–841.
20 W. Cheng, X. -F. Zhou and R. G. Compton, *Angew.Chem. Int. Ed.*, 2013, **52**, 12980-12982.
21 X. Xiao and A. J. Bard, J. Am. Chem. Soc., 2007, **129**, 9610-9612.
22 X. Xiao, F. -R. F. Fan, J. Zhou and A. J. Bard, *J. Am. Chem. Soc.*, 2008, **130**, 16669-16677.
23 J. H. Park, S. N. Thorgaard, B. Zhang and A. J. Bard, *J. Am. Chem. Soc.*, 2013, **135**, 5258-5261.
24 H. Zhou, J. H. Park, F. -R. F. Fan and A. J. Bard, *J. Am. Chem. Soc.*, 2012, **134**, 13212-13215.

RSC Advances Accepted Manuscript


This journal is © The Royal Society of Chemistry 20xx

Please do not adjust margins




25 S. J. Kwon and A. J. Bard, *J. Am. Chem. Soc.*, 2012, **134**, 10777-10779.
26 A. Bonanni, M. Pumera and Y. Miyahara, *Phys. Chem. Chem. Phys.*, 2011, **13**, 4980.
27 Y. -G. Zhou, N. V. Rees, J. Pillay, R. Tshikhudo, S. Vilakazi and R. G. Compton, *Chem. Commun.*, 2012, **48**, 224-226.
28 D. Lin, J. Wu, F. Yan, S. Deng and H. Ju, *Anal. Chem.*, 2011, **83**, 5214-5221.
29 Y. Zhu, P. Chandra and Y. -B. Shim, *Anal. Chem.*, 2013, **85**, 1058-1064.
30 W. Niu, S. Zheng, D. Wang, X. Liu, H. Li, S. Han, J. Chen, Z. Tang and G. Xu, *J. Am. Chem. Soc.*, 2009, **131**, 697–703.
31 C. L. Cleveland, U. Landman, T. G. Schaaff, M. N. Shafigullin, P. W. Stephens and R. L. Whetten, *Phys. Rev. Lett.*, 1997, **79**, 1873-1876.
32 H. Häkkinen, *Nature Chem.*, 2012, **4**, 443-455.
33 J. F. Hicks, A. C. Templeton, S. Chen, K. M. Sheran, R. Jasti, R. W. Murray, J. Debord, T. G. Schaaff and R. L. Whetten, *Anal. Chem.*, 1999, **71**, 3703-3711.
34 S. Chen and R. W. Murray, *J. Phys. Chem. B*, 1999, **103**, 9996-10000.
35 S. Chen, *Langmuir*, 1999, **15**, 7551-7557.
36 S. Chen, R. W. Murray and S. W. Feldberg, *J. Phys. Chem. B*, 1998, **102**, 9898-9907.


RSC Advances Accepted Manuscript

## Graphical Abstract

In the communication, we assembled an electroactive *p*-hydroxythiophenol (*p*-HTP) monolayer on a gold nanoparticle surface and produced an amplified single particle-collision electrochemical signal, thus allowing us to sensitively detect the size and functions of inert gold particles in aqueous solution.

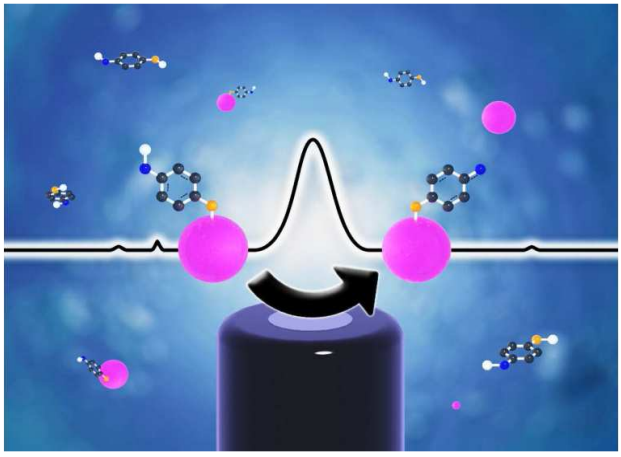

RSC Advances Accepted Manuscript